

INTERDECADAL VARIABILITY OF WESTERN NORTH PACIFIC TROPICAL CYCLONE ACTIVITY

Kin Sik Liu and Johnny C. L. Chan *

Laboratory for Atmospheric Research, Department of Physics and Materials Science
City University of Hong Kong, Hong Kong, China

1. INTRODUCTION

It is well known that tropical cyclone (TC) activity over the western North Pacific (WNP) exhibits interannual and interdecadal variations (Chan and Shi 1996; Yumoto and Matsuura 2001; see also Fig. 1a). The former has been extensively investigated by many researchers. The occurrence of the El Niño-South Oscillation phenomenon has been shown to result in significant modifications of various respects of TC activity (Chan 1985, 2000; Wang and Chan 2002; Camargo and Sobel 2005), the results of which have been used in the statistical seasonal prediction of annual TC activity (Chan et al. 1998).

On the other hand, relatively fewer studies have been carried out on the interdecadal variations of TC activity and their physical connection to other known decadal climatic variations. Matsuura et al. (2003) found a significant relationship between the interdecadal variability of TC activity and the long-term variations of the zonal wind stresses in the tropical WNP and the sea-surface temperatures (SSTs) in the tropical western and central North Pacific (NP). Ho et al. (2004) investigated the interdecadal variations of summertime (June–September) typhoon tracks in the WNP. While these studies have identified the interdecadal variations of TC activity and their possible relationships with the long-term variations of some oceanic and atmospheric conditions, very few studies have tried to relate the former with the large-scale decadal climatic oscillations or to develop seasonal forecast schemes based on factors with decadal variations. The objective of this study is thus to investigate the possible relationship between the atmospheric and oceanic conditions over the NP and the annual TC activity on interdecadal time scales.

2. DATA

2.1 Tropical cyclone data

TC data for the WNP during the period 1962–2004 are obtained from the website of the Joint Typhoon Warning Center (www.npmoc.navy.mil/jtwc/best_tracks/). The annual TC activity is defined as the annual number of tropical storms and typhoons (maximum sustained 1-minute mean surface winds $\geq 17 \text{ m s}^{-1}$ for tropical storm and $\geq 33 \text{ m s}^{-1}$ for typhoon). Only TCs that reached at least tropical storm intensity are considered to minimize subjectivity in the identification of weak systems. TC data before the 1960s are not used because of possible missing TCs.

2.2 Oceanic and atmospheric fields

NOAA Extended Reconstructed SST data are obtained from the NOAA-CIRES Climate Diagnostics Center. The horizontal resolution of the dataset is 2° latitude \times 2° longitude. Monthly atmospheric fields are extracted from the European Centre for Medium-Range Weather Forecasts ERA-40 dataset. The horizontal resolution of the dataset is 2.5° latitude \times 2.5° longitude.

3. LONG-TERM VARIATIONS OF ANNUAL TC ACTIVITY

The time series of the annual TC activity exhibits interannual and interdecadal variations (Fig. 1a). Applying the sequential method of regime shift detection developed by Rodionov (2004) to this time series, two active periods (1962–74 and 1989–97) and two inactive periods (1975–88 and 1998–2004) can be identified. The annual TC activity during the period 1962–74 is generally high, with a mean number of 29.3. The activity is relatively low during the period 1975–88 with a mean number of 24.7 but becomes much higher again during the period 1989–1997, with all the years having above-normal annual TC activity except 1995. The annual TC activity appears to be lower after 1998. The differences in annual TC activity between successive periods are statistically significant at the 95% confidence level.

* Corresponding author address: Prof. Johnny Chan, Dept. of Physics and Materials Science, City University of Hong Kong, Tat Chee Ave., Kowloon, Hong Kong, China.
E-mail: Johnny.Chan@cityu.edu.hk

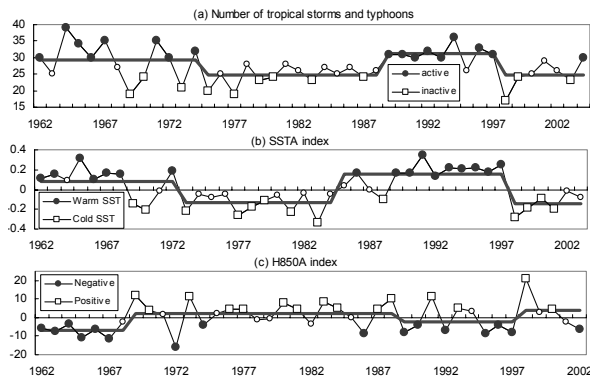


Fig. 1. Time series of (a) the annual TC activity, (b) SSTA index and (c) H850A index. The stepwise functions indicate the regime shifts with the cutoff length of 10 years and significance levels of 0.1 for (a) and (b) and 0.5 for (c).

4. TROPICAL SST ANOMALIES

4.1 Relationship with annual TC activity

Annual TC activity is found to have a statistically-significant positive correlation with the March–May SST anomalies in the tropical NP between 160°E and 150°W (Fig. 2a). The correlation between the SST anomaly averaged within the area 8° – 14°N , 170°E – 155°W (to be defined as the SSTA index hereafter) and the annual TC activity is 0.65, which is statistically significant at the 99% confidence level. Positive SSTA index is generally found during the period 1962–72 except for the years 1969 and 70 (Fig. 1b). Then the SSTA index becomes negative during the period 1973–85. It becomes positive again after 1986 but switch back to negative after 1998.

To examine further such a SST–TC activity relationship, a year is classified as warm (cold) SST year if the SSTA index is ≥ 0.1 (≤ -0.1), which corresponds to about half of its standard deviation. The mean annual TC activities for warm (17 cases) and cold (13 cases) SST years are 30.5 and 23.5 respectively and the difference is statistically significant at the 99% confidence level.

4.2 North Pacific SST patterns

The characteristic SST patterns of the NP are identified first through the Empirical Orthogonal Function (EOF) analysis and their association with the SST anomalies in the tropical central NP is then examined.

The first EOF (Fig. 3a) explains $\sim 37\%$ of the total variance and reveals the typical SST pattern associated with the Pacific Decadal Oscillation (PDO, Mantua et al. 1997). Indeed, the first principal component (PC1) is highly correlated ($r = 0.86$) with the March–May PDO index. Negative loadings are found over the

central NP between 25°N and 45°N , with the maximum amplitude at about 35°N , 160°W , while positive loadings are found along the west coast of North America, which extend to the central NP south of 25°N . This pattern is generally in its negative phase during the period 1962–77 but changes to its positive phase during the period 1978–98 (Fig. 3d). Its phase becomes negative again after 1999.

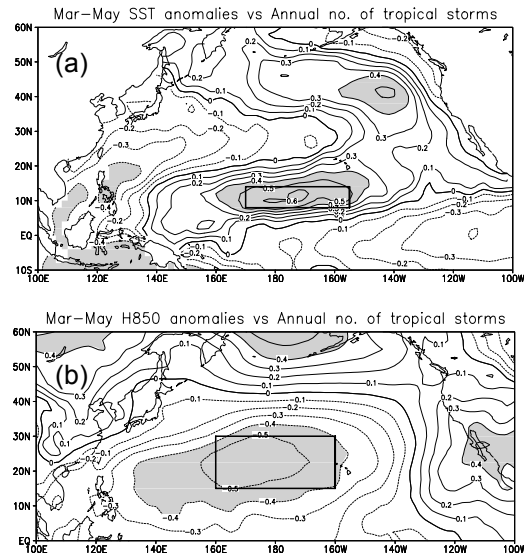


Fig. 2. Correlation map for the annual TC activity and (a) the Mar–May SST anomalies and (b) 850-hPa geopotential height anomalies. Shadings indicate the correlation is significant at the 99% confidence level. Boxes in (a) and (b) indicate the regions 8° – 14°N , 170°E – 155°W and 15° – 30°N , 160°E – 160°W respectively.

The second EOF (Fig. 3b), which explains $\sim 20\%$ of the total variance, represents the Victoria pattern (Bond et al. 2003). Negative loadings are found over the subtropical (20°N – 35°N) NP west of 160°W and an arc of opposite sign is found along 40°N extending to the subtropical central NP. The EOF2 SST pattern is in its positive phase during the period 1962–1974 (Fig. 3e) but is apparently not significant during the period 1975–1997 except for a few individual years. After 1998, it becomes prominent again and is in its negative phase.

The third EOF, which explains $\sim 14\%$ of the total variance, shows alternate east–northeast–west–southwest oriented regions of positive and negative loadings, with the former extending from 45°N , 135°W to 25°N , 120°E and the latter extending from 35°N , 130°W to 15°N , 140°E (Fig. 3c). Note that positive loadings are also found between 8°N and 15°N east of 170°E . The PC3 shows a large fluctuation during the period 1962–73 (Fig. 3f). This pattern is in its negative phase during the period 1974–88 but changes to positive phase after 1989.

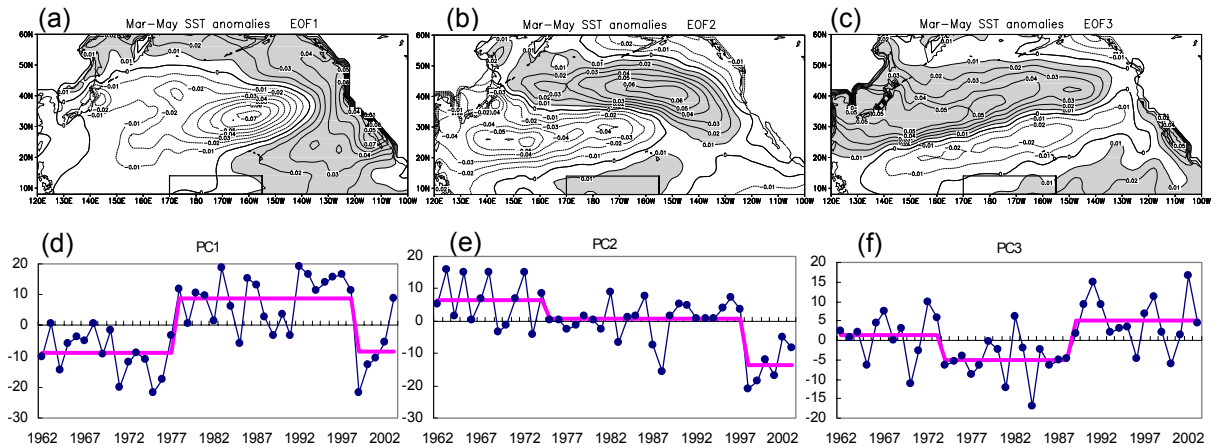


Fig. 3. The spatial patterns of the Mar–May SST anomalies for (a) EOF1, (b) EOF2 and (c) EOF3. The sign of the EOF is chosen such that it is positively correlated with the SSTA index. Areas with value > 0.01 are shaded. The box indicates the region 8° – 14° N, 170° E– 155° W. Time series of (d) PC1, (e) PC2 and (f) PC3.

The SST patterns and the time coefficients of the three EOFs suggest that the positive SSTA index during 1962–72 are mainly associated with the positive phase of the EOF2 SST pattern (Fig. 3e). Then the negative phase of the EOF1 and EOF3 SST patterns dominates the period 1973–85, with the former dominates years 1973–76 and the latter dominates years 1977–85 (Figs. 3d and 3f). The NP is then dominated by the positive phase of the EOF1 and EOF3 SST patterns during 1986–97 (Figs. 3d and 3f). The oceanic condition of the NP reverses after 1998 as the EOF1 and EOF2 SST patterns shift to the negative phase (Figs. 3d and 3e) and hence the negative SSTA index.

5. ATMOSPHERIC CIRCULATION ANOMALIES

5.1 Relationship with TC activity

The correlation map for the March–May 850-hPa geopotential height anomalies and the annual TC activity shows a north-south dipole with positive correlations over the Bering Sea and negative correlations over the subtropical NP centered at about 25° N, 175° E (Fig. 2b). Indeed, the mean value over the area 15° – 30° N, 160° E– 160° W (to be defined as the H850A index hereafter) is highly correlated with the annual TC activity, with a correlation coefficient of -0.58 , which is statistically significant at the 99% confidence level. The H850A index is negative during the period 1962–68 (Fig. 1c), becomes generally positive between 1969 and 1988 but then switches back to negative between 1989 and 1997. After 1998, it becomes positive again.

The H850A index is classified as positive (negative) phase if its value is ≥ 3.5 (≤ -3.5), which corresponds to about half of its standard deviation. The mean annual TC activities for

negative (16 cases) and positive (15 cases) H850A years are 30.8 and 24.1 respectively and the difference is statistically significant at the 99% confidence level.

5.2 NP atmospheric circulation pattern

The first EOF of the anomalous March–May 850-hPa geopotential height field (Fig. 4a) explains $\sim 44\%$ of the total variance and reveals the typical anomalous atmospheric circulation pattern associated with the PDO (Mantua et al. 1997), as demonstrated by the significant correlation between the PC1 and the March–May PDO index ($r = -0.66$). Positive loadings, which represent the strength of the Aleutian Low (Overland et al. 1999), are found over the extratropical NP centered at about 50° N, 165° W while negative loadings are found over the subtropical NP south of 30° N although the magnitude is smaller. This mode is generally in its positive phase during 1962–68 but shows a large fluctuation during 1969–78 (Fig. 4d). Starting from 1979, it is generally in its negative phase but appears to become positive again after 1999.

The second EOF, which explains $\sim 22\%$ of the total variance, resembles a north-south dipole with a positive center over the Bering Sea and a negative center over the central NP centered at about 38° N, 155° W (Fig. 4b). Such a pattern is similar to the East Pacific-North Pacific (EP-NP) pattern (defined by the Climate Prediction Center, NOAA). Indeed, the time coefficient of this mode is highly correlated with the mean March–May EP-NP index ($r = 0.77$). The EOF2 pattern is generally in its positive phase during 1962–72 but switches to the negative phase during 1973–88 (Fig. 4e). The period 1989–97 is then dominated by the positive phase.

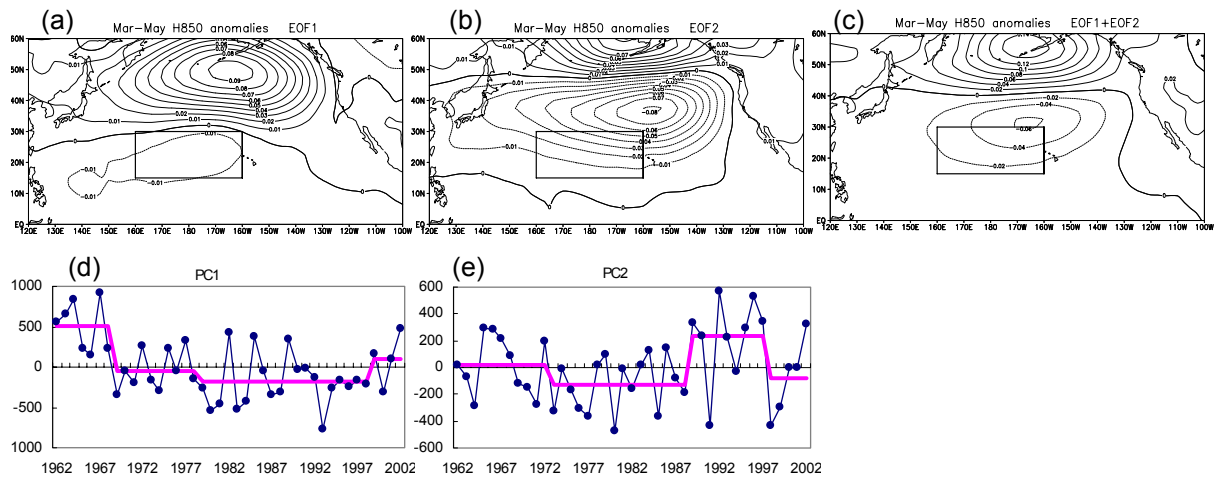


Fig. 4. The spatial patterns of the Mar–May 850-hPa geopotential height anomalies for (a) EOF1, (b) EOF2 and (c) a combination of EOF1 and EOF2. The sign of the EOF is chosen such that it is negatively correlated with the H850A index. The box indicates the region 10° – 15° N, 160° E– 160° W. Time series of (d) PC1 and (e) PC2.

The springtime anomalous atmospheric circulation pattern over the NP is mainly related to the variability of the monopole associated with the PDO (EOF1 pattern), the dipole associated with the EP–NP pattern (EOF2 pattern), or a combination of them (referred as EOF1+2 pattern hereafter). The latter has a similar pattern with the EOF2 pattern except that the dipole shifts southward, with the southern center displacing from around 40° N to around 30° N (Fig. 4c). In the early and middle 1960s, the positive phase of the EOF1 pattern dominates the NP (Fig. 4d). Then the NP is mainly dominated by the negative phase of the EOF1, EOF2 or EOF1+2 patterns during 1969–1988. The period 1989–97 is then dominated by the positive phase of the EOF2 pattern (Fig. 4e). The H850A index can be considered as a single indicator of the phase of these patterns and can well represent the anomalous atmospheric circulation and has an appreciable relationship with the annual TC activity.

6. THE PHYSICAL LINK TO TC ACTIVITY

6.1 Spring (March–May)

To understand the relationship between the SSTA and H850A indices and the annual TC activity, the oceanic and atmospheric conditions from spring to peak TC season are examined. The springtime conditions favorable for active TC season are summarized in Figure 5. Warmer SSTs are generally found in the tropical central NP, indicating the positive phase of the SST patterns described in section 4b. A dipole of 850-hPa geopotential height anomaly, with a positive center at 55° N, 170° W and a negative center at 28° N, 175° W, is found over the NP. At the same time, enhanced low-level easterlies occur between the cyclone and the anticyclone

along 40° N and statistically-significant westerly anomalies are also observed over the tropical western and central NP, which may be related to the coupled ocean-atmosphere system associated with SST patterns and the anomalous atmospheric circulation patterns. Opposite signs of these anomalies are linked to inactive TC seasons.

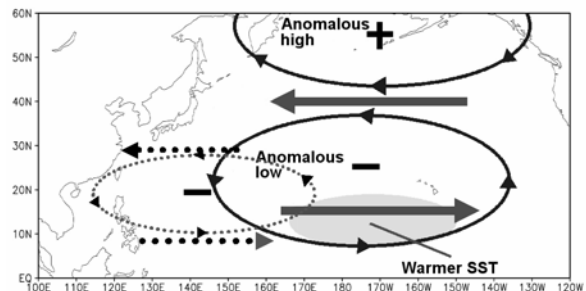


Fig. 5. Schematic diagram of the oceanic and atmospheric conditions of the North Pacific favorable for annual TC activity. Ellipse represents the anomalous low-level circulation during March–May (Solid) and July–October (dotted), with minus sign indicating the anomalous low center and plus sign indicating the anomalous high center. Arrow represents the zonal wind anomaly during March–May (Solid) and July–October (dotted). Shaded area indicates the warmer SSTs.

6.2 TC season (July–October)

As TC activity is primarily linked to the strength and position of the monsoon trough, which is associated with the strength of the subtropical high and the trade winds, the atmospheric conditions related to TC genesis are examined. The SST anomalies in the tropical central NP established in spring apparently persist into the TC season, with the July–October SST being significantly correlated

with that in March–May ($r = 0.74$). The north-south pressure dipole weakens significantly but the anomalous anticyclone over the subtropical WNP persists into the peak TC season. In addition, the subtropical high is weaker. These oceanic and atmospheric conditions generally give westerly anomalies over the tropical WNP, which lead to positive 850-hPa relative vorticity anomalies over the subtropical WNP. The stronger monsoon trough provides favorable atmospheric condition for TC genesis and therefore higher annual TC activity is generally observed.

7. SUMMARY

This study investigates the relationship between the interdecadal variation of the WNP annual TC activity and the springtime oceanic and atmospheric conditions of the NP. The annual TC activity shows significant interdecadal variations, with active periods during 1962–75 and 1989–97 and inactive period during 1976–88. The interdecadal variation of the annual TC activity is partly linked to the decadal variability of the NP and the overlying atmosphere, which can be reflected by the March–May SST anomalies in the area 8° – 14° N, 170° E– 155° W (SSTA index) and the 850-hPa geopotential height anomalies in the area 15° – 30° N, 160° E– 160° W (H850A index). Negative (positive) H850A index and positive (negative) SSTA index are generally associated with active (inactive) annual TC activity.

The March–May SST pattern is largely related to the EOF1 (PDO pattern), EOF2 (Victoria pattern) and EOF3 of the anomalous SST field while the anomalous atmospheric circulation pattern is mainly related to the EOF1 (PDO pattern) and EOF2 (EP-NP pattern) of the anomalous 850-hPa geopotential height field. The phase and the magnitude of these patterns can be reflected by the SSTA and H850A indices respectively. These indices also serve as the proxies for the atmospheric conditions over the WNP during the TC season.

Positive SST anomalies in the tropical central NP and a north-south dipole of the 850-hPa geopotential height anomalies, with a positive center in the north and a negative center in the south, over the NP are generally associated with active TC season. Such anomalies generally persist into the peak TC season and lead to an anomalous cyclone over the subtropical WNP and westerly anomalies over the tropical WNP. As a result, the stronger monsoon trough and weaker subtropical high lead to the favorable atmospheric conditions for the TC formation over the tropical WNP.

Acknowledgments. This research is supported by City University of Hong Kong Grant 9610021.

REFERENCES

- Bond, N. A., J. E. Overland, M. Spillane and P. Stabeno, 2003: Recent shifts in the state of the North Pacific. *Geophys. Res. Lett.*, **30** (23), 2183, doi:10.1029/2003GL018597.
- Camargo, S. J. and A. H. Sobel, 2005: Western North Pacific tropical cyclone intensity and ENSO. *J. Climate.*, **18**, 2996–3006.
- Chan, J. C. L., 1985: Tropical cyclone activity in the northwest Pacific in relation to El Niño/Southern Oscillation phenomenon. *Mon. Wea. Rev.*, **113**, 599–606.
- , 2000: Tropical cyclone activity over the western North Pacific associated with El Niño and La Niña events. *J. Climate*, **13**, 2960–2972.
- and J. E. Shi, 1996: Long-term trends and interannual variability in tropical cyclone activity over the western North Pacific. *Geophys. Res. Lett.*, **23**, 2765–2767.
- , — and C. M. Lam, 1998: Seasonal forecasting of tropical cyclone activity over the western North Pacific and the South China Sea. *Wea. Forecasting*, **13**, 997–1004.
- Ho, C. H., J. J. Baik, J. H. Kim, D. Y. Gong and C. H. Sui, 2004: Interdecadal changes in summertime typhoon tracks. *J. Climate*, **17**, 1767–1776.
- Mantua, N. J., S. R. Hare, J. M. Wallace and R. C. Francis, 1997: A Pacific decadal climate oscillation with impacts on salmon production. *Bull. Amer. Meteor. Soc.*, **78**, 1069–1079.
- Matsuura, T., M. Yumoto and S. Iizuka, 2003: A mechanism of interdecadal variability of tropical cyclone activity over the western North Pacific. *Climate Dyn.*, **21**, 105–117.
- Overland, J. E., J. M. Adams and N. A. Bond, 1999: Decadal variability of the Aleutian low and its relation to high-latitude circulation. *J. Climate*, **12**, 1542–1548.
- Rodionov, S. N., 2004: A sequential algorithm for testing climate regime shifts. *Geophys. Res. Lett.*, **31**, doi:10.1029/2004GL019448.
- Wang, B. and J. C. L. Chan, 2002: How strong ENSO events affect tropical storm activity over the western North Pacific. *J. Climate*, **15**, 1643–1658.
- Yumoto, M. and T. Matsuura, 2001: Interdecadal variability of tropical cyclone activity in the western North Pacific. *J. Meteor. Soc. Japan*, **79**, 23–35.